Light-induced molecular adsorption and reorientation at polyvinylcinnamate-fluorinated/liquid-crystal interface

O. Francescangeli, L. Lucchetti, F. Simoni, and V. Stanić
Dipartimento di Fisica e Ingegneria dei Materiali e del Territorio and Istituto Nazionale per la Fisica della Materia, Università Politecnica delle Marche, Via Brecce Bianche, 60131 Ancona, Italy

A. Mazzulla
Licryl-Liquid Crystals Laboratory, Istituto Nazionale per la Fisica della Materia c/o Dipartimento di Fisica, Università della Calabria, 87036 Arcavacata di Rende (CS), Italy
(Received 30 July 2004; published 6 January 2005)

We have carried out a detailed experimental study, by means of x-ray reflectometry (XRR) and half-leaky guided mode (HLGM) optical characterization, of the light-induced molecular adsorption and reorientation at the polyvinylcinnamate-fluorinated (PVCN-F)/liquid-crystal (LC) interface of a LC cell doped with the azo-dye methyl red (MR). The XRR data allowed characterizing the microscopic structure of the adsorbed dye layer both before irradiation (*dark* adsorption) and after irradiation (light-induced adsorption). The HLGM optical characterization has made possible the experimental determination of the nematic director profile in the LC cell and evaluation of the effects of light-induced adsorption on the LC anchoring conditions. The experimental findings have confirmed the formation of a dark-adsorbed layer and are in agreement with the absorption model previously proposed to account for the complex phenomenology related to light-induced anchoring and reorientation in dye-doped liquid crystals.

DOI: 10.1103/PhysRevE.71.011702 PACS number(s): 61.30.Hn, 68.43.−h, 42.70.Df, 61.10.Kw

I. INTRODUCTION

Light-induced reorientation phenomena in liquid crystals (LC's) have been widely investigated over the last two decades for both fundamental and technological reasons [1]. Within this wide outline, dye-doped liquid crystals (DDLC's) play a special role mainly related to the enhanced sensitivity of the LC to light irradiation due to the active role of the dye [2]. Interest in DDLC's has greatly expanded in recent years because of the high potentiality of these materials for applications in molecular microassembly [3], nonlinear and adaptive optics [4,5], optical information storage and processing [6–8].

Photoalignment effects in DDLC's were first observed in LC's doped with azo-dyes [9,10]. The most intriguing aspects of photoalignment is the possibility of generating an easy-orientation axis with consequent stable director alignment over a nonphotosensitive isotropic boundary surface of a LC cell, upon irradiation by polarized laser light [10,11]. This mechanism offers the possibility of regulating the amount of anchoring energy under control of the incident light [12]. The value of light intensity needed to align or reorient the LC director in the DDLC cells is among the smallest ever observed: energy densities on the order of $0.1\ \mathrm{J/cm^2}$ were sufficient to write both high-resolution holographic gratings [6,7] and binary images [8]. In these pioneering experiments planar LC cells were used in which one boundary glass surface (the *reference* surface) was coated with a polyimide layer mechanically rubbed to provide strong homogeneous planar anchoring, while the second boundary surface (the *command* surface) was coated with an untreated isotropic layer of fluorinated polyvinyl-cinnamate (PVCN-F), providing negligibly small azimuthal anchoring. The cells were filled with a mixture of the commercial nematic liquid crystal 5CB and the azo-dye Methyl Red (MR) at $\approx 1\%$ weight concentration. A complex reorientation phenomenology involving the superposition of bulk and surface effects was observed upon irradiation of the command surface with polarized laser light [11]. In particular, it was observed that light illumination induces fast transient quasifree sliding of the molecular director, followed by its permanent reorientation. Originally it was proposed that a bulk torque due to reorientation of the MR molecules promoted by the *trans-cis* photoisomerization of the azo-dye was responsible for the fast reorientation outward the exciting polarization. On the other hand, the formation of the easy axis parallel to the exciting polarization was interpreted in terms of anisotropic adsorption of the MR dichroic molecules onto the illuminated surface during light irradiation within the dye's adsorption band (light-induced adsorption effect) [1,6,11]. Later on, the adsorption-driven photoalignment effect was studied in the isotropic phase [13] where the LC order parameter is zero and therefore the surface director orientation cannot affect the direction along which dye molecules are adsorbed. Besides dye adsorption, this investigation pointed to a further effect playing a role in the reorientation process—namely, the photoinduced anisotropic desorption of dye molecules in the adsorbed layer. Within this scheme the experimental results were interpreted assuming that after filling the LC cell, a thin layer of adsorbed MR molecules grows over the PVCN-F surface (*dark* adsorption). Subsequent irradiation with polarized laser light in the isotropic phase, followed by slow cooling to the mesophase, results in the development of surface anisotropy in this dark-adsorbed layer with consequent easy-axis generation, due to concomitant action of light-induced desorption of dark-adsorbed MR

molecules and light-induced adsorption of MR molecules located in the vicinity of the surface. The direction of the easy axis can be either parallel or perpendicular to the exciting polarization depending on which of the two processes (adsorption or desorption, respectively) prevails, which in turn is dictated by the intensity of the incident light [13]. Also the results of a next extensive investigation of the light-induced reorientation in LC cells irradiated in the nematic phase could be successfully interpreted in terms of competition between adsorption and desorption effects [14]. More recent experiments have demonstrated that this phenomenology is quite general, being responsible for director reorientation even in the transient regime [15]. These experiments strongly support the model of adsorption and desorption of MR molecules, as responsible for the modifications of the surface anchoring conditions that are believed to originate the recently discovered surface-induced nonlinear effect (SINE) [16,17] and the related extraordinarily large [4] and colossal optical nonlinearities [18] in DDLC's (i.e., nonlinear refractive index $\approx 10^3$ cm^2/W, about 10^{14} times the values found in good conventional Kerr media). Finally, the fast reorientation induced by a single 4-ns laser pulse of low energy in a MR-doped nematic LC cell [19] was also interpreted in terms of light-induced modification of the surface anisotropy resulting from anisotropic MR-adsorption and desorption processes [19].

In spite of this large body of experimental work, only very few attempts have been made so far to get direct experimental evidence of dye adsorption, mainly through polarizing microscopy and atomic force microscopy (AFM) [3]. In this work we report the results of an experimental study carried out by means of x-ray reflectometry (XRR) and optical characterization by the half-leaky guided-mode (HLGM) technique, aimed at (i) testing the adsorption-desorption model, (ii) characterizing the microscopic structure of the adsorbed dye layer, (iii) measuring the effects of light-induced adsorption on the LC anchoring conditions, and (iv) determining the profile of the reoriented LC director over the bulk of the LC cell. The results confirm the previously proposed adsorption model and provide the first quantitative determination of the structural properties of the dye-adsorbed layers as well as of the effects of the light-induced anchoring modifications on the macroscopic LC director orientation.

II. EXPERIMENT

A. Sample preparation

The experiments were performed using the commercial nematic pentyl-cyanobiphenyl 5CB (from Merck) doped with the azo-dye MR (from Aldrich) at weight concentration $c_{MR} \approx 0.5\%$. MR dissolved in nematic 5CB assumes the azo form [3,20]. The photosensitive 5CB-LC mixture was used to fill a combined parallel-plane cell [11,13,14].

The combined LC cell was assembled from pairs of commercial glass plates coated with transparent electroconductive layers of indium tin oxide (ITO). One of the two ITO-coated glass surfaces (the *reference* surface) was covered by a thin layer of polyimide by means of spin coating. This layer was then mechanically rubbed to get uniaxial strong homogeneous planar anchoring (i.e., parallel to the rubbing direction). The command surface was realized by coating the second glass plate with a thin film of PVCN-F. PVCN-F consists of a maim chain polyvinyl alcohol endowed with photosensitive side groups based on fluorinated cinnamic acid [21]. The PVCN-F layer was deposited by spreading a solution of the polymer onto the ITO-coated glass substrate followed by spin coating for 30 s at 3000 rpm speed. The concentration $c=1\%$ of the polymer in the solvent (a mixture 50%-50% of dichloroethane and dichlorobenzene) was chosen considering the recent results of a morphological study by AFM of the surface of PVCN-F layers spin coated under our identical experimental conditions [22]. According to this study, deposition of a continuous layer of PVCN-F that completely covers the substrate requires a minimum concentration of $\cong 0.75\%$. On the other hand, concentrations higher than $\cong 2\%$ result in strongly inhomogeneous and rough PVCN-F surfaces. The film obtained after spin coating was backed at 80 °C for 30 min. Then the layer was exposed for 5 min to unpolarized UV light from Hg lamp. This irradiation promoted cross linking of the polymer chains that made the polymer surface rigid and prevented the polymer from dissolving in the LC. The cell was then assembled with the glass plates facing their polymer-coated sides in a parallel-plane configuration and being separated by Mylar spacers to get precise control the cell thickness L ($L=17$ μm). Finally the cell (1 cm$\times$1 cm) was filled with the LC photosensitive 5CB-MR mixture by capillarity in the isotropic phase and then slowly cooled down to room temperature. In this way we got uniform planar alignment of the LC in the cell, with the nematic director parallel to the direction imposed by the strong-anchoring rubbed-polyimide surface (indicated as the *reference* direction in the following). Figure 1(a) shows a schematic representation of a cross section of the LC cell.

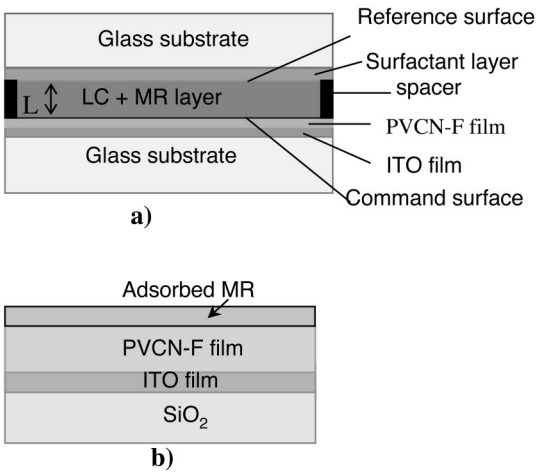

FIG. 1. (a) Schematic representation of the LC cell used in the experiments. The surfactants used in XRR and HLGM measurements are different. In the former case it is a thin layer of rubbed polyimide, in the latter case it consists of a SiO_x film deposited under vacuum. Both surfactants provide strong homogeneous planar anchoring. (b) Cross section of the multilayered structure probed by XRR from the side of the command surface, as obtained after disassembling the LC cell and washing for the residual LC.

After filling, the cell was irradiated with linearly polarized light from an Ar^+ laser ($\lambda = 514$ nm, $I = 100$ mW/cm^2) impinging normally onto the glass plates from the side of the command surface. The irradiation time was 3600 s. The whole surface (1 cm $\times$ 1 cm) was irradiated in order to get homogeneous alignment of the LC. Several identical cells were prepared following the same procedure, which were then irradiated with the Ar^+ laser beam polarized at different angles with respect to the reference direction ($\Phi = 0, \pi/4, \pi/2$). After irradiation, light-induced reorientation on the command surface was probed by means of the optical pump-probe technique described in Refs. [11,13,14].

For the XRR characterization of the command surface, the cells were disassembled after irradiation and the thin layer of LC remaining over the PVCN-F substrate was washed away by warm (40 °C) hexane [3]. This procedure allowed us to remove any trace of the LC without altering the adsorbed dye layer, as proved by infrared absorption spectroscopy. A sketch of the cross section of the disassembled LC cell used for the XRR study is shown in Fig. 1(b). An additional nonirradiated LC cell was also prepared and disassembled as described above to be used as reference sample for the XRR measurements.

A slight different assembly of the LC cell was used for the HLGM measurements. In fact, the HLGM technique [23] needs strict conditions on the refractive indices of the boundary glass plates. In order to fulfill these requirements, the PVCN-F film was deposited by spin coating on a fused-silica (FS) low-refraction index glass substrate ($n = 1.4570$ at $\lambda = 633$ nm) coated with a thin layer of ITO. The PVCN-F layer was deposited, then backed, and finally exposed to unpolarized UV light as previously described. The planar reference surface consisted of a SiO_x film deposited under vacuum at 60° evaporation angle on a ITO-coated high-index glass plate (SF10, $n = 1.7231$ at $\lambda = 633$ nm) to get a strong homogeneous planar-anchoring layer. The cell was then assembled using Mylar spacers to give 17 μm thickness and filled with the 5CB-MR (0.5%) photosensitive mixture. We performed HLGM measurements before and after irradiation of the LC cell by the Ar^+ laser beam ($I = 30$ mW/cm^2, irradiation time = 3600 s) polarized at an angle $\Phi = \pi/4$ with respect to the reference direction.

B. XRR measurements

Specular XRR measurements were carried out by means of the Bruker D8-Advance reflectometer using Cu $K\alpha$ radiation ($\lambda = 1.54$ Å). A sketch of the experimental geometry is shown in Fig. 2.

Specular XRR at an ideally flat plane interface separating two media with different uniform electron densities is described by the Fresnel laws of classical optics. The refractive index for x rays is given by

$$n = 1 - \delta - i\beta, \tag{1}$$

with $\delta = \lambda^2 r_e \rho_e / 2\pi$ and $\beta = \lambda\mu/4\pi$, where r_e is the classical electron radius, ρ_e is the electron density of the material, and μ is the linear absorption coefficient. When the sample has more than one interface (like multilayered systems), interference of the waves reflected at all interfaces give rise to intensity oscillations in the reflectivity curve (*Kiessig* fringes), whose frequencies allow determination of the thickness of each single layer contributing to the reflection. The experimental XRR data were analyzed by means of the REFSIM simulation software package (by Bruker-AXS) which makes use of the Parrat formalism [24] to model the multilayer structure. In this software, microscopic surface and interface roughness are taken into account within the Nèvot-Croce model [25,26]: the interface at z_0 (the z axis being along the surface normal) is represented by an ensemble of smooth interfaces whose positions are distributed around z_0 following a Gaussian distribution:

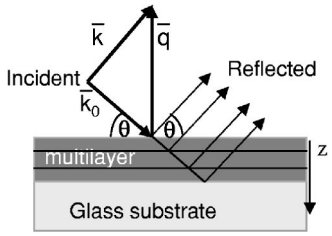

FIG. 2. Geometry of the x-ray reflectivity measurements. The incident monochromatic x-ray beam (wave vector $\mathbf{k}_0$) impinges on the sample at grazing angle θ and is specular reflected to wave vector $\mathbf{k}$. The scattering vector $\mathbf{q} = \mathbf{k} - \mathbf{k}_0$ ($q = 4\pi \sin\theta/\lambda$) lies along the surface normal.

$$w(z) = \frac{1}{\sqrt{2\pi\sigma}} \exp[-(z - z_0)^2/2\sigma^2], \tag{2}$$

where the standard deviation σ represents the rms roughness. Structural and physical parameters (i.e., thickness, roughness, mass and electron densities, linear absorption coefficient of each single layer) were obtained by best fitting the reflectivity curve calculated from the model density to the experimental data.

C. HLGM measurements

Optical excitation of half-leaky guided modes is a technique that has been successfully used in recent years to characterize in detail the optical tensor profile [23,27–29] in a LC layer. The power of this technique when applied to a LC cell is the full determination of the LC director profile in the cell. In the present study the HLGM technique was used with the aim of gaining the full optical characterization of the cell, including the nematic director profile, before and after irradiation. The experimental setup is shown in Fig. 3(a). The LC cell consists of a thin layer (17 μm) of the 5CB-MR mixture sandwiched between the high-index glass plate and the low-index glass substrates described in the previous section. The orientation of the nematic director **n** at any given point in the LC cell is defined by the tilt angle θ, between **n** and the layer normal, and the twist angle ϕ, between the projection of **n** over the command surface and the reference direction [i.e., the y axis; see Fig. 3(b)]. Light is coupled into the system via an index-matched prism. In this geometry, there exists a small angular range encompassed by a pseud-

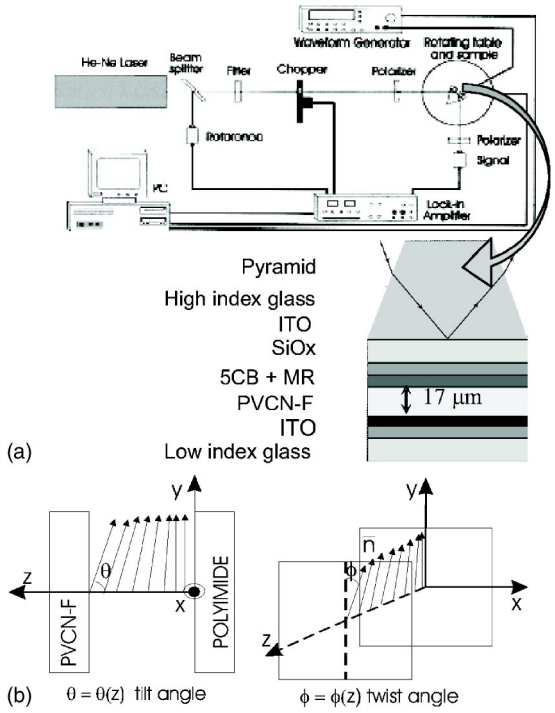

FIG. 3. (a) Experimental setup for the optical characterization of the LC cell by means of the HLGM optical technique. (b) Schematic representation of the nematic director orientation in the LC cell; θ and ϕ are the tilt and twist angles, respectively.

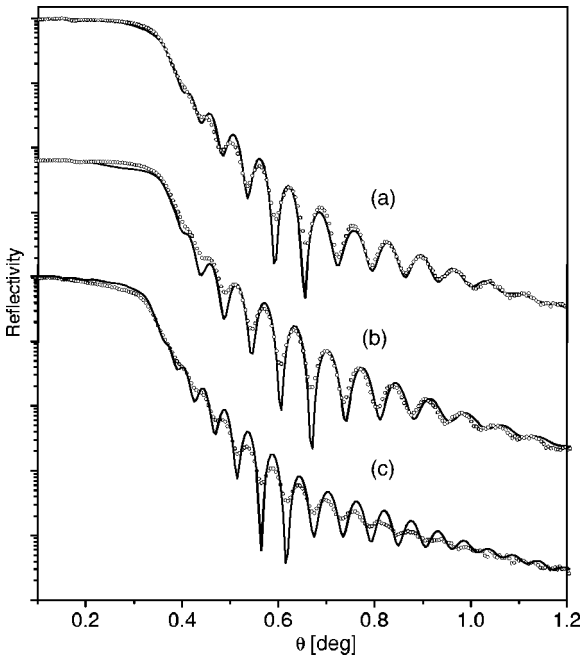

FIG. 4. X-ray reflectivity data (open circles) vs the grazing angle, θ, for the following layered systems: (a) SiO_2/ITO/PVCN-F; (b) SiO_2/ITO/PVCN-F/MR, before irradiation; (c) SiO_2/ITO/PVCN-F/MR, after irradiation with Ar^+ laser beam linearly polarized at 45° to the reference direction. The solid lines are the best fit to the experimental data.

ocritical angle and a critical angle, associated with the pyramid-LC and pyramid-glass substrate boundaries, respectively, over which sharp half-leaky resonant guided modes may propagate [23]. For any director twist out of the incident plane a significant TM (p) to TE (s) conversion occurs in the cell. Then, within the above angular window the p-to-s conversion gives rise to sharp resonant features in the angle-dependent optical reflectivity, which are remarkably sensitive to the director profile in the cell.

These reflectivity peaks are sharp because the optical field is fully reflected at the LC-substrate boundary while being relatively strongly reflected at the high-index glass-LC boundary. Also by measuring the p-to-s (or s-to-p) conversion signals that result from the director being out of the plane of incidence, the technique becomes in effect of higher order than measurement of the simple p-to-p or s-to-s reflectivity. This thereby allows a detailed characterization of the optical tensor profile in the cell. In order to collect experimental data in the form of prism-LC boundary reflectivity vs incidence angle, the complete cell is placed on a computer-controlled rotation stage. A He—Ne laser beam ($\lambda = 632.8$ nm), modulated at 960 Hz to allow phase-sensitive detection, impinges on one face of the prism such that it reaches the LC layer at the desired angle of incidence. The incident beam is plane polarized, either s or p, and a second polarizer is placed in front of the detector to give either p or s signal component. To allow for any variation in the laser source intensity, a small reflection is taken from the input beam to act as a reference. In these measurements, experimental data were taken with the SiO_x alignment direction in the plane of incidence. The four angle-dependent reflectivity curves so obtained, R_{ss}, R_{pp}, R_{sp} and R_{ps}, were fitted (simultaneously for the four data sets, to avoid degeneracy of the solution) to Fresnel model predictions based on a reasonable *a priori* profile of the nematic director.

The Fresnel multilayer modeling uses a scattering matrix method [30] with the LC layer divided into 50 or more sublayers, depending on the tilt angle gradient. Berreman's 4×4 matrix technique is used in the modeling. A reasonable hypothesis is first made of all the cell optical parameters and the director profile. This produces a model prediction of the reflectivity that is compared with the data. Adjustments are then iteratively made to all the parameters until a minimum least-squares fit to the data is obtained, giving a complete evaluation of the optical structure.

III. RESULTS AND DISCUSSION

A. XRR measurements

XRR measurements and related data analysis were carried out in accordance with the following scheme. First the ITO-coated glass was characterized by XRR before and after deposition with PVCN-F, in order to get reliable reference values of the unknown structural parameters to be set in the next data analysis. Figure 4(a) (open circles) shows a representative example of the experimental data collected for the PVCN-F/ITO-coated glass substrate. The best fit to these data is shown by the solid line of Fig. 4(a) and the corresponding fit parameters are listed in Table I. The thickness of the PVCN-F layer is about 24 nm with a rms roughness of

TABLE I. Structural data obtained from the fit of the XRR data for the SiO_2/ITO/PVCN-F-layered structure.

Layer	d [nm]	σ [nm]	ρ [g/cm^3]	β [$\times 10^{-6}$]	δ [$\times 10^{-6}$]
PVCN-F	23.7	2.2	1.20	0.009	4.02
ITO	56.7	1.7	7.14	1.680	20.13
SiO_2		0.6	2.50	0.105	8.10

2.2 nm. Several PVCN-F layers deposited following the same procedure were characterized in order to test the reproducibility of the deposition technique. All these measurements gave values of the PVCN-F layer thickness in the range between 20 and 35 nm, with a rms roughness between 1 and 3 nm. We note that such values of surface roughness are in good agreement with those observed by AFM in similar PVCN-F layers [22].

After characterization of the command surface the LC cell was assembled and filled with the LC mixture. Before studying the effects of light irradiation this cell was disassembled, the remnants of LC over the command surface (PVCN-F layer) were washed away as described in the experimental section and then the command surface was characterized by XRR. This procedure allowed us the direct probing and microscopic structural characterization of the MR layer adsorbed in the absence of irradiation (i.e., the dark adsorbed layer). Figure 4(b) (open circles) shows the corresponding reflectivity data together with the best fit curve (solid line). The values of the model parameters resulting from the refinement procedure are listed in Table II. These were obtained from the REFSIM simulation procedure, using the data of Table I as starting values of the model parameters for the SiO_2, ITO, and PVCN-F layers and allowing variation of all the parameters. The substantial coincidence, within the experimental errors, of the values of the variables common to the two refinements (Tables I and II) represents a strong confirmation the reliability of the fitting procedure. XRR data confirm the existence of a dark-adsorbed layer and provide a precise measure of the thickness, $d=5.6$ nm, and of the rms roughness of its surface, $\sigma=1.9$ nm. Measurements performed under the same experimental conditions on a number of identically prepared samples gave values of the layer thickness between 3.5 nm and 6 nm with a rms roughness around 2 nm. From the measured values of thickness, $d=5.6$ nm, and density, $\rho_{MR}=1.13\times 10^3$ kg/m^3, of the MR layer we could estimate the surface density of adsorbed dye molecules—i.e., the number of MR molecules adsorbed per unit area of the command surface. The mass m_{mol} of the dye molecule was calculated from the molar mass $M=269.3\times 10^{-3}$ kg/mol and the Avogadro number $N_A=6.02\times 10^{23}$ as $m_{mol}=M/N_A=4.47\times 10^{-25}$ kg. The surface density of adsorbed molecules is then $N=d\times\rho_{MR}/m_{mol}=1.43\times 10^{15}$ cm^{-2}. On the other hand, the surface density of MR molecules (i.e., number of molecules per unit area of the command surface) initially dissolved in the LC cell is $N_{dis}\cong L\times\rho_{MR}\times c_{MR}/m_{mol}=4.29\times 10^{16}$ cm^{-2}. Then, the ratio $N/N_{dis}=1/30\cong 3\%$ gives the number fraction of the overall MR molecules involved in the dark-adsorption process.

TABLE II. Structural data obtained from the fit of the XRR data for the SiO_2/ITO/PVCN-F/MR-layered structure before irradiation.

Layer	d [nm]	σ [nm]	ρ [g/cm^3]	β [$\times 10^{-6}$]	δ [$\times 10^{-6}$]
MR	5.6	1.9	1.13	0.005	3.91
PVCN-F	22.2	1.0	1.26	0.009	4.22
ITO	55.4	1.7	7.14	1.679	20.13
SiO_2		0.6	2.50	0.105	8.10

TABLE III. Structural data obtained from the fit of the XRR data for the SiO_2/ITO/PVCN-F/MR-layered structure after irradiation at 45°.

Layer	d [nm]	σ [nm]	ρ [g/cm^3]	β [$\times 10^{-6}$]	δ [$\times 10^{-6}$]
MR	51.6	5.9	1.03	0.005	3.55
PVCN-F	33.4	1.0	1.20	0.009	4.17
ITO	69.0	1.8	6.14	1.440	17.32
SiO_2		0.6	2.50	0.105	8.10

For the study of light-induced adsorption an identical LC cell was assembled and irradiated with polarized laser light as described in the experimental section. The cell was then disassembled, the command surface was washed by warm hexane to remove any trace of the LC, and finally the surfaced was investigated by XRR. Figure 4(c) (open circles) shows the reflectivity data corresponding to the incident light beam polarized at 45° to the reference planar orientation imposed by the rubbed polyimide layer. The best fit curve is also shown by the solid line in the same figure and the corresponding fit parameters are reported in Table III. The differences in the model parameters of SiO_2, ITO, and PVCN-F between Tables II and III are explained considering that, because of the previous disassembling, the irradiated cell was necessarily distinct from that used for the dark-adsorption characterization. The relevant data of Table III concern the adsorbed MR layer: a layer thickness of about 52 nm is found with a surface rms roughness of $\cong 6$ nm. This finding is extremely important as it clearly relates the grown of the dye adsorbed layer with the irradiation process. In other words, the experimental results unambiguously prove the occurrence of a light-induced adsorption process that leads to a significant growth of the preexisting adsorbed dye layer (the dark-adsorbed layer). Based on these results, an increase of the dye-adsorbed layer thickness from 5.6 nm to 51.6 nm (i.e., of a factor around 10) occurs upon irradiation. This corresponds to an equivalent increase of the surface density of adsorbed molecules. In fact, with $d=51.6$ nm and a density $\rho_{MR}=1.03\times 10^3$ kg/m^3, a calculation analogous to that for the dark-adsorbed layer gives a surface density of adsorbed dye molecules, $N=d\times\rho_{MR}/m_{mol}=1.19\times 10^{16}$ cm^{-2}. This value corresponds to a ratio $N/N_{dis}=1/3.6\cong 30\%$ indicating that a big fraction of the overall number of dye molecules dissolved in the LC mixture participates in the adsorp-

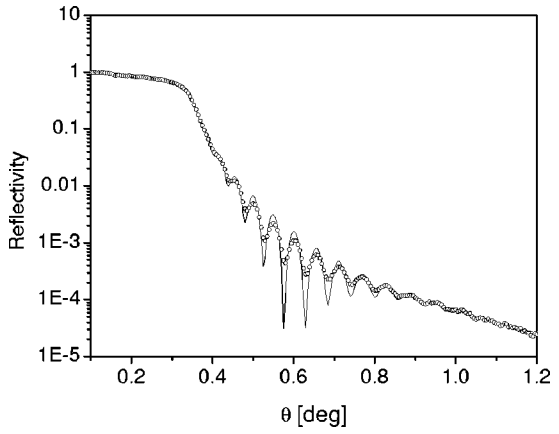

FIG. 5. X-ray reflectivity data (open circles) vs the grazing angle, θ, for the four-layer SiO_2/ITO/PVCN-F/MR structure, after irradiation with Ar^+ laser beam linearly polarized at 90° to the reference direction. The solid line is the best fit to the experimental data.

tion process. Thus, the formation of the light-induced adsorbed layer involves bulk processes such as molecular transport and spatial redistribution of the dye.

Light-induced adsorption was also observed in a LC cell after irradiation with laser light polarized at a different angle—i.e., 90°—to the reference planar orientation. Figure 5 shows the corresponding reflectivity data together with the best fit curve whereas the relevant fit parameters are collected in Table IV. Also in this case an increase of the adsorbed-layer thickness is observed upon irradiation, even though to a lower extent. In fact, the initial 5.6-nm-thick dark-adsorbed layer grows up to 10.3 nm after irradiation. As will be discussed in the next section, Sec. III B, all these result are in agreement with the adsorption model proposed to explain the observed photoinduced reorientation phenomena in DDLC's [13,14].

B. HLGM measurements

Optical characterization by the HLGM technique allowed us to get a detailed description of the nematic director profile in the LC cell. In order to evaluate the effects of light irradiation, two series of measurements on the same LC cell were carried out, before and after irradiation.

Figures 6 and 7 (dots) show the four experimental reflectivity curves R_{pp}, R_{ss}, R_{ps}, and R_{sp} versus internal incident angle, measured before and after irradiation, respectively. The recorded data were fitted using a software based on the Fresnel multilayer modeling, as described in the experimental section. Worthy of note, the simultaneous fit of the four reflectivity data sets represents an extremely stringent condition on the model parameters, which makes very high the reliability of the results of the data elaboration. The data fit allowed us obtaining also the optical parameters of all layers shown in the LC cross section of Fig. 1(a). Figures 8 and 9 show the profile of the twist and tilt angles of the nematic director in the LC cell before and after irradiation, respectively, corresponding to the best fit shown by the solid lines of Figs. 6 and 7. The relevant model fit parameters of the LC listed in the first row of Table V. We observe that the ordinary, n_o, and extraordinary, n_e, refractive indexes of the DDLC take values very close to the corresponding values of the pure LC (i.e., $n_o=1.542$ and $n_e=1.728$). As concerns the output fit parameters of the other layers, here we note only that the ITO thickness, 105 nm, coincides with the value supplied by the factory, the parameters relative to SiO_x take the typical values known for this material [29], and the PVCN-F layer thickness compares favorably with the XRR analysis. For the MR layer we obtained a refraction index of 1.5. As concerns the MR layer thickness, an increment from $d\cong 6$ nm for the dark-adsorbed layer to $d\cong 60$ nm for the light-induced adsorbed layer was found, which confirms the light-induced growth of the adsorbed layer, in close agreement with the previous XRR data.

TABLE IV. Structural data obtained from the fit of the XRR data for the SiO_2/ITO/PVCN-F/MR-layered structure after irradiation at 90°.

Layer	d [nm]	σ [nm]	ρ [g/cm^3]	β [$\times 10^{-6}$]	δ [$\times 10^{-6}$]
MR	10.3	0.9	0.90	0.004	3.28
PVCN-F	35.5	3.3	1.20	0.007	3.98
ITO	67.3	2.2	6.65	1.564	18.76
SiO_2		0.6	2.58	0.109	8.36

Another important result of the HLGM optical analysis is the finding of a tilted configuration of the nematic director in the cell before irradiation, as evidenced by Fig. 8. In particular, a linear profile of the tilt angle is found along the cell thickness, varying between $\theta=71.6°$ (at the command surface) and $\theta=90°$ (at the reference surface). Accordingly, a pretilt angle $\gamma=90°-\theta$ of 18.4° is present before irradiation at the PVCN-F surface whereas a zero pretilt (i.e., planar anchoring) occurs at the polyimide surface. On the other hand, no twist of the nematic director is present in the LC cell before irradiation, as shown by the uniform zero-valued twist angle profile of Fig. 8.

Figure 9 shows the nematic director profile in the LC after irradiation. A strong effect of the irradiation on the anchoring conditions at the command surface is apparent comparing Figs. 8 and 9. In fact, after irradiation the pretilt angle at the command surface disappears and the tilt takes the uniform zero-valued profile of Fig. 9. On the other hand, the twist angle at the command surface after irradiation becomes $\phi=39.5°$ and the twist exhibits the linear behavior shown in Fig. 9. Whereas due to the strong anchoring energy no change is observed upon irradiation at the reference surface, big changes of the anchoring conditions are observed at the reference surface due to the light action. Based on the above results, light-induced adsorption at the command surface reorients the nematic director over the command surface at an angle of 39.5° with respect to the reference direction and changes the azimuthal anchoring of the LC. Due to the elastic properties of the LC, the nematic director reorientation at the command surface finally results is the uniform planar-twisted configuration of Fig. 9. These aspects will be further discussed in the next section with specific reference to the

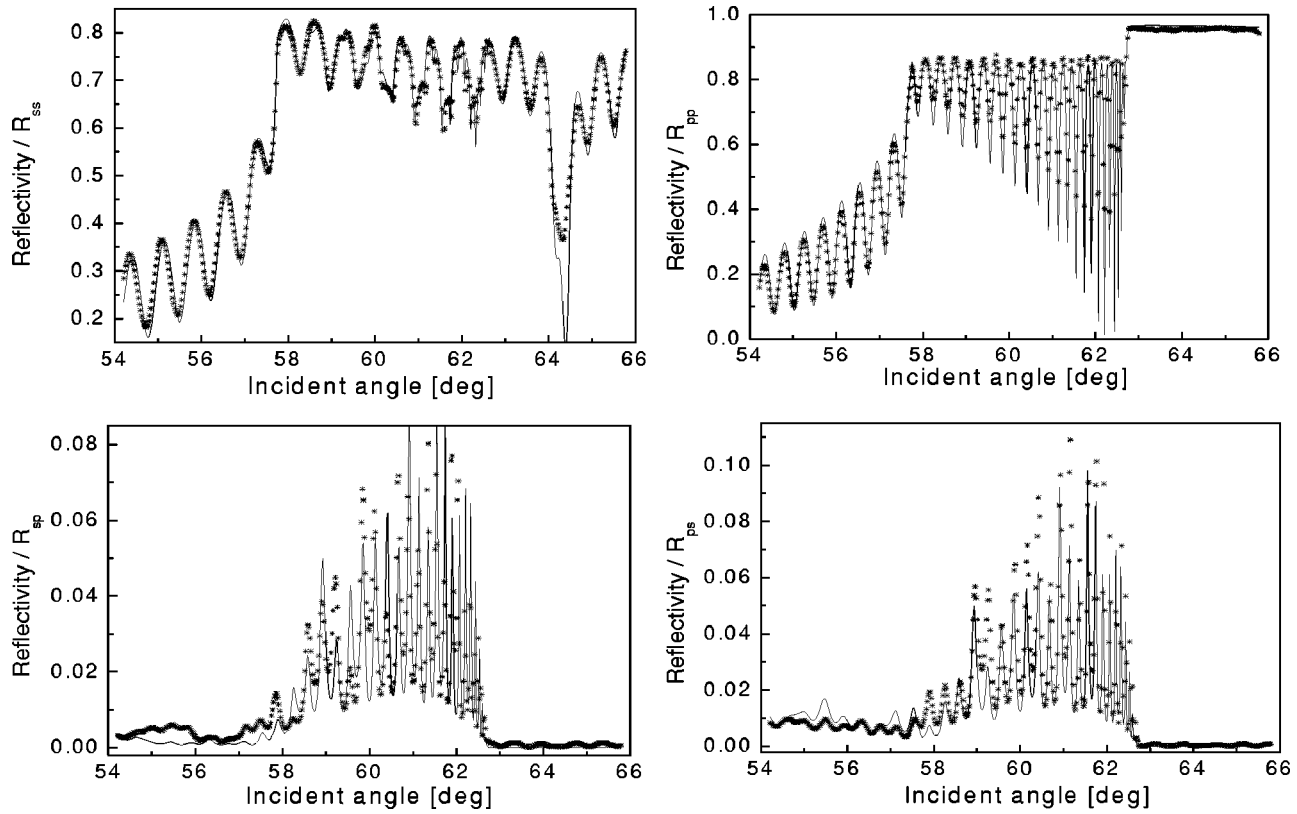

FIG. 6. The four experimental reflectivity curves (dots) R_{ss}, R_{pp}, R_{sp}, and R_{ps} vs the internal angle of incidence, before irradiation, measured by the HLGM technique. The solid linear are the best fit to the experimental data.

light-induced formation of an easy axis over the command surface.

C. Discussion

The experimental results of the previous paragraphs provide a strong support to the kinetic approach [13,14] proposed to explain the observed photoinduced reorientation phenomena in DDLC's [13,14]. This approach considers deposition of dye as a relaxation process toward a stationary state, controlled by adsorption and desorption processes both affected by light. The motion of dye molecules is considered as Brownian diffusion in the potential field. This field exists near the surface due to van der Waals and electrostatic interactions. Specific LC effects caused by the orientational and translational order parameter changes may also contribute to this potential. The characteristic time of adsorption before illumination (dark adsorption) is much longer than the characteristic time of dye diffusion over the cell, and the order parameter increases near the surface. This suggests that the field repulses dye molecules from the surface, and they have to overcome this barrier to reach the surface. Light irradiation in the absorption band excites the dye molecules and affects the adsorption process through the following mechanisms. First, the nonradioactive relaxation of the dye excitation after light absorption results in the local heating of the LC region in the vicinity of the absorbing molecules. In addition, reverting to the ground state, dye molecules may change their geometry (*trans-cis* isomerization). Both effects reduce the potential barrier for adsorption near the surface. Second, light absorption by bulk dye molecules close to the surface stimulates the adsorption process. Third, light absorption by dye molecules belonging to the adsorbed layer stimulates the desorption process. The competition between light-induced effects in adsorption (first two mechanisms) and desorption (the third one) results in the different stationary surface concentrations of adsorbed molecules at different irradiation intensities.

Based on this model, after filling the cell a layer of dark-adsorbed MR molecules with axially symmetric orientation grows over the PVCN-F surface. The adsorption and desorption processes determine the equilibrium thickness of this layer. Light action changes this equilibrium thickness and violates the axial symmetry. Because of strong absorption dichroism the dye molecules participating in the light-induced adsorption and desorption processes are predominantly oriented along the direction of light polarization **E**. Therefore, light-induced desorption decreases the density of adsorbed molecules parallel to **E** and orients the easy axis perpendicular to **E**. At the same time, light-induced adsorption increases the density of adsorbed molecules parallel to **E** and orients the easy axis parallel to **E**. Thus, a light-induced increase of the dye adsorbed layer thickness produces a reorientation toward **E** whereas a light-induced layer decrease reorients the director outward **E**. Which of the two processes controls the final orientation of the easy axis depends on the intensity of the incident light. At low intensities light-induced anisotropy in the adsorbed MR layer prevails

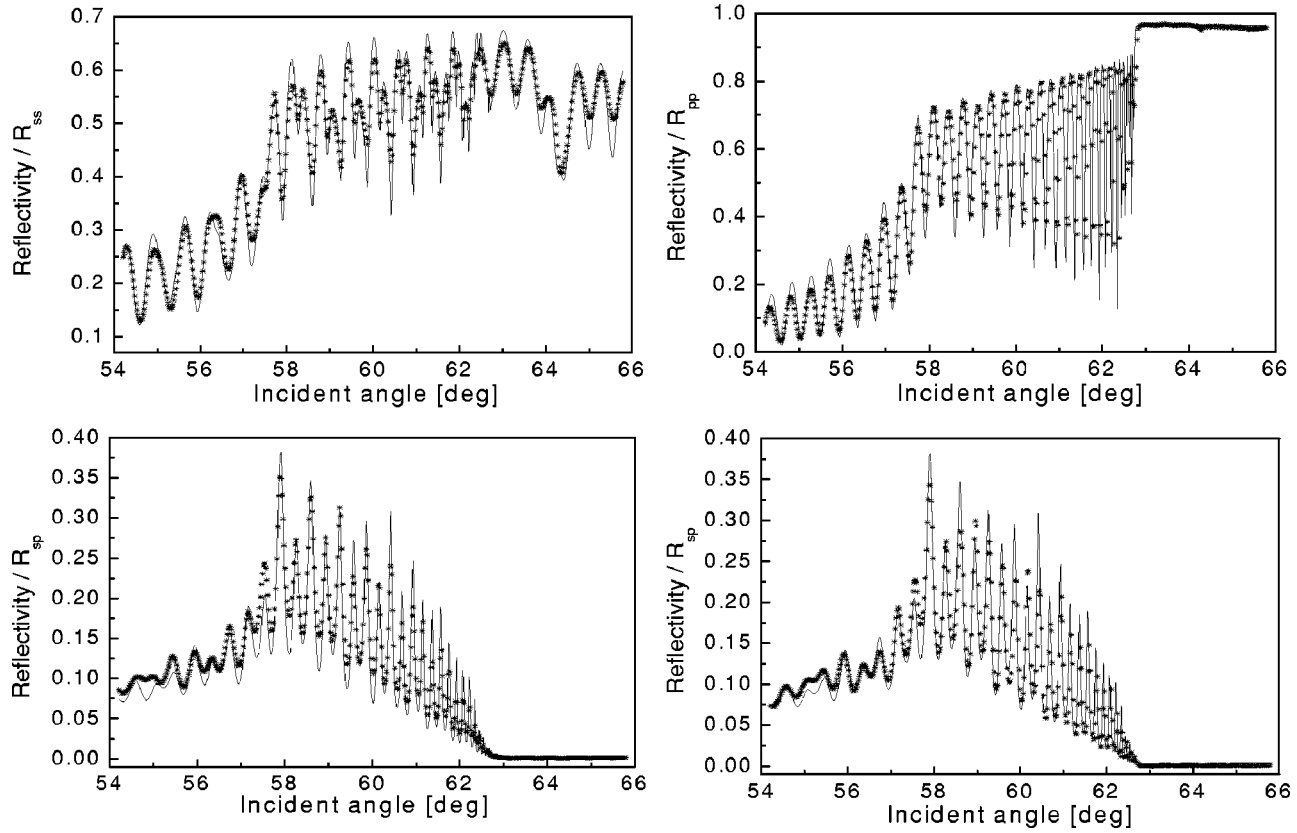

FIG. 7. The four experimental reflectivity curves (dots) R_{ss}, R_{pp}, R_{sp}, and R_{ps} vs the internal angle of incidence, after irradiation with Ar^+ laser beam linearly polarized at 45°, measured by the HLGM technique. The solid linear are the best fit to the experimental data.

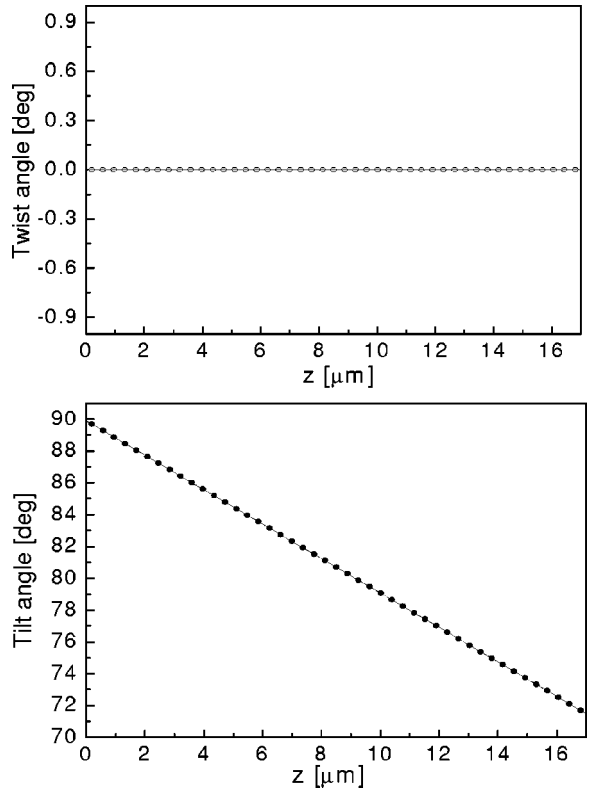

FIG. 8. The profiles of the twist and tilt angles of the nematic director in the LC cell before irradiation.

whereas at high intensities light-induced adsorption dominates.

In agreement with the above model, XRR data unambiguously prove the existence of a dark-adsorbed layer which forms upon filling the LC cell. Even though very thin (5–6 nm) this layer is enough extended to include an appreciable fraction (3%) of the dye molecules initially dissolved in the LC mixture. As consequence of the irradiation with light polarized at 45°, a great increase of the adsorbed layer thickness is measured by XRR. In addition, the HLGM optical characterization reveals a reorientation of the nematic director over the LC bulk, driven by the light-induced rotation of the director on the command surface towards the incident polarization **E**. The measured twist angle at the command surface, $\phi = 39.5°$, is very close to the polarization angle of the incident wave field **E** ($\Phi = 45°$). This experimental evidence is easily interpreted within the kinetic approach considering that, in our experimental conditions, light-induced adsorption prevails over desorption. In such conditions the growth of the dye-adsorbed layer increases the density of adsorbed molecules parallel to **E**, leading to the onset of an easy axis possibly oriented along **E**. The lower value of ϕ compared to Φ is to be ascribed to a preexisting *dark* easy axis at the command surface which forms after filling the cell and before irradiation [14]. This axis is generated by the *anisotropic* dark adsorption of dye molecules due to the orientational order parameter of the LC which makes the MR molecules near the surface predominantly oriented parallel to the reference direction.

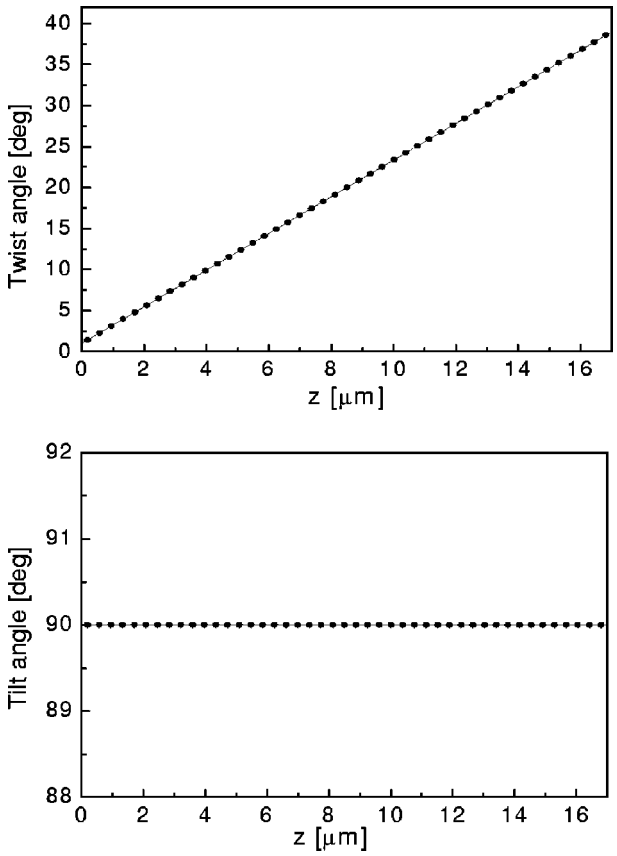

FIG. 9. The profiles of the twist and tilt angles of the nematic director in the LC cell after irradiation with Ar^+ laser beam linearly polarized at 45°.

Within this picture we can also interpret the results of the XRR measurements after irradiation with light polarized at 90° to the reference direction. In fact, because of the same irradiation intensity, adsorption is expected to prevail over desorption, leading to an increase of the dye-adsorbed layer thickness. However, due to the relatively high orientational order of the MR molecules in the LC (order parametere $S_{MR} \approx 0.35$), dye molecules before irradiation are predominantly oriented parallel to the reference orientation—i.e., orthogonal to the incident polarization. Due to the strong absorption dichroism of the MR molecules [31], light irradiation is mostly effective for molecules oriented parallel to the exciting polarization, which results in a reduced number of excited dye molecules and then a reduced number of adsorbed molecules. On the other hand, also the desorption process is less effective because of the preferential orientation of the dark-adsorbed molecules parallel to the reference

TABLE V. The relevant parameters of the DDLC obtained from the fit of the HLGM reflectivity data.

Irradiation	n_o	n_e	Twist (SiO_x)	Twist (PVCN-F)	Tilt (SiO_x)	Tilt (PVCN-F)
Before	1.532	1.707	0°	0°	90°	71.6°
After	1.533	1.708	0°	39.5°	90°	90°

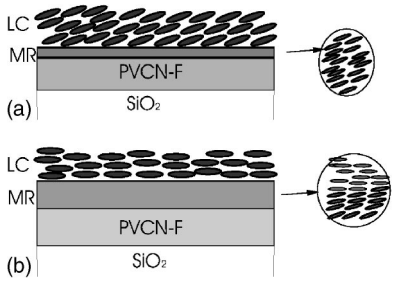

FIG. 10. Schematic representation of the polar anchoring of the LC at the PVCN-F command surface in the presence of a (a) dark-adsorbed MR layer and (b) light-induced adsorbed MR layer. The strong effects of irradiation on the anchoring conditions is clearly apparent comparing the two figures.

direction (due to the above discussed anisotropic nature of the dark-adsorption process). The final consequence of the reduced adsorption and desorption is the modest growth of the adsorbed layer, much smaller than obsrved at 45° of polarization.

A final aspect which deserves further consideration is the light-induced modification of the polar anchoring boundary conditions over the command surface. The HLGM optical analysis clearly shows the existence of a pretilt of the nematic director, which disappears after irradiation. The measured value of the pretilt over the command surface is quite typical of PVCN/LC interfaces [32]. The tilted alignment of a pure LC on a PVCN surface was first observed by Dyadyusha *et al.* [33] who proposed a model according to which the cinnamate side groups are responsible for oblique orientation. More recent experiments [32] have pointed out also the important role of the surface polarity in the mechanism of pretilt generation. Based on our experimental evidence, deposition of the thin dark-adsorbed MR layer on the PVCN-F surface does not change appreciably the pretilt angle of the LC whereas the formation of the thicker light-induced adsorbed layer changes dramatically the polar anchoring condition, reducing to zero the pretilt angle. A tentative explanation of this result can be proposed considering the role of orientation and order of the adsorbed molecules in connection with the ability of the LC to mimic the orientational structure of the solid interface. This latter aspect has been recently investigated by combined XRR and ellipsometry techniques [34], showing that the ordering tendency can be effectively transferred from polymer bulk to polymer surface and then to LC if the symmetry is not lost at the polymer-LC interface. In our situation it is easy to imagine that the efficiency of the ordering transfer from the PVCN-F surface to the LC is mainly determined by the order of the dye adsorbed-layer that actually plays the role of polymer/LC interface. On the other hand, molecular orientation and order in the adsorbed layer depend on the competition between photoinduced adsorption and self-organization processes. Based upon these considerations, the following model can be proposed as summarized in Fig. 10. Dark adsorption leads to deposition of a thin layer of MR molecules with their long axis preferentially oriented along the tilted direction imposed by the PVCN-F surface. In this way, the tilt ordering tendency is transferred from the polymer to the

LC via the dye-adsorbed layer [Fig. 10(a)]. Upon irradiation, light-induced adsorption grows a thicker dye layer where the tilted orientational order of the molecules is progressively lost and the molecules adsorb with the long axis preferentially oriented parallel to the command surface. In this case, the adsorbed dye layer is thick enough to *shield* the LC from the PVCN-F surface and to orient the LC parallel to the command surface [Fig. 10(b)]. Consistent with this picture, a less efficient packing of the molecules is expected in the light-induced adsorbed layer, which should result in a lower mass density compared to the dark-adsorbed one, as experimentally found (see Tables II and III).

IV. CONCLUSIONS

We have studied the dark- and light-induced adsorption of MR molecules on PVCN-F plane surfaces by means of XRR and HLGM optical characterization. Combined XRR and HLGM have provided a unique tool to fully characterize the light-induced adsorption and reorientation effects in DDLC's. The XRR data allowed characterizing the microscopic structure of the dye adsorbed layer in terms of layer thickness, surface roughness, and mass and electron densities. Worthy of note, this represents the first experimental determination of such properties for the dye-adsorbed layer of a LC cell. The HLGM optical characterization has made possible the experimental determination of the nematic director profile in the LC cell before and after irradiation and evaluation of the effects of light-induced adsorption on the LC anchoring conditions.

The results have confirmed the existence of a dark-adsorbed layer and are in agreement with the absorption model previously proposed to account for the complex phenomenology related to light-induced anchoring and reorientation effects in DDLC's. However, a full confirmation of the model requires a further step consisting in the XRR study of the PVCN-F surface under experimental conditions in which the light-induced desorption prevails over adsorption. In this case, XRR analysis should reveal a reduction of dye-adsorbed layer thickness upon irradiation. In addition to this, a complete combined XRR and HLGM study as a function of both direction and polarization of the incident light would provide important additional information to fully validate the model. These studies will be the subject of future investigations.

ACKNOWLEDGMENTS

It is our pleasure to thank Dr. D. Federenko for assistance in the sample preparation. The authors acknowledge financial support from INFM within the PAIS-LIMAD project (No. 2002-2003).

[1] F. Simoni and O. Francescangeli, J. Phys.: Condens. Matter **11**, R439 (1999).
[2] I. Jánossy, A. D. Lloyd and B. S. Wherrett, Mol. Cryst. Liq. Cryst. **179**, 1 (1990).
[3] D. Voloschenko and O. D. Lavrentovich, J. Appl. Phys. **86**, 4843 (1999).
[4] I. C. Khoo, S. Slussarenko, B. D. Günther, M. Y. Shih, P. Chen, and M. V. Wood, Opt. Lett. **23**, 253 (1998).
[5] L. Lucchetti, M. D. Fabrizio, M. Gentili, and F. Simoni, Appl. Phys. Lett. **83**, 5389 (2003).
[6] F. Simoni, O. Francescangeli, Y. Reznikov, and S. Slussarenko, Opt. Lett. **22**, 549 (1997).
[7] S. Slussarenko, O. Francescangeli, F. Simoni, and Y. Reznikov, Appl. Phys. Lett. **71**, 3613 (1997).
[8] I. C. Khoo, M. Shih, M. V. Wood, B. D. Günther, P. Chen, F. Simoni, S. Slussarenko, O. Francescangeli, and L. Lucchetti, Proc. IEEE **87**, 1897 (1999).
[9] S. T. Sun, W. M. Gibbons, and P. J. Shannon, Liq. Cryst. **12**, 869 (1992).
[10] D. Voloshchenko, A. Khyzhnyak, Y. Reznikov, and V. Reshetnyak, Jpn. J. Appl. Phys., Part 1 **34**, 566 (1995).
[11] O. Francescangeli, S. Slussarenko, F. Simoni, D. Andrienko, V. Reshetnyak, and Y. Reznikov, Phys. Rev. Lett. **82**, 1855 (1999).
[12] O. Francescangeli, D. E. Lucchetta, S. Slussarenko, Y. Reznikov, and F. Simoni, Mol. Cryst. Liq. Cryst. Sci. Technol., Sect. A **360**, 193 (2001).
[13] E. Ouskova, D. Fedorenko, Y. Reznikov, S. V. Shiyanovskii, L. Su, J. L. West, O. V. Kuksenok, O. Francescangeli, and F. Simoni, Phys. Rev. E **63**, 021701 (2001).
[14] E. Ouskova, Y. Reznikov, S. V. Shiyanovskii, L. Su, J. L. West, O. V. Kuksenok, O. Francescangeli, and F. Simoni, Phys. Rev. E **64**, 051709 (2001).
[15] L. Lucchetti, M. D. Fabrizio, O. Francescangeli, and F. Simoni, J. Nonlinear Opt. Phys. Mater. **11**, 13 (2002).
[16] F. Simoni, L. Lucchetti, D. E. Lucchetta, and O. Francescangeli, Opt. Express **9**, 85 (2001).
[17] L. Lucchetti, D. E. Luchetta, O. Francescangeli, and F. Simoni, Mol. Cryst. Liq. Cryst. Sci. Technol., Sect. A **375**, 641 (2002).
[18] L. Lucchetti, M. D. Fabrizio, O. Francescangeli, and F. Simoni, Opt. Commun. **233**, 417 (2004).
[19] L. Lucchetti, D. Fedorenko, O. Francescangeli, Y. Reznikov, and F. Simoni, Opt. Lett. **28**, 1621 (2003).
[20] S. Yamamoto, N. Nishimura, and S. Hasegawa, Bull. Chem. Soc. Jpn. **46**, 194 (1973).
[21] A. Reiser, *The Science and Technology of Resists in Photoreactive Polymers* (Wiley, New York, 1989).
[22] I. Gerus, A. Glushchenko, S. B. Kwon, V. Reshetnyak, and Y. Reznikov, Liq. Cryst. **28**, 1709 (2001).
[23] F. Yang and J. R. Sambles, J. Opt. Soc. Am. B **10**, 858 (1993).
[24] L. G. Parrat, Phys. Rev. **95**, 359 (1954).
[25] L. Nèvot and P. Croce, Rev. Phys. Appl. **15**, 761 (1980).
[26] B. Vidal and P. Vicent, Appl. Opt. **23**, 1794 (1984).
[27] F. Yang and J. R. Sambles, Mol. Cryst. Liq. Cryst. Sci. Technol., Sect. A **250**, 143 (1994).
[28] A. Mazzulla and J. R. Sambles, Liq. Cryst. **22**, 727 (1997).
[29] A. Mazzulla, F. Ciuchi, and J. R. Sambles, Phys. Rev. E **64**, 021708 (2001).

[30] D. Y. K. Ko and J. R. Sambles, J. Opt. Soc. Am. A **5**, 1863 (1988).
[31] H. Rau, in *Photochemistry and Photophysics*, edited by F. J. Rabeck (Boca Raton, Florida, 1990), Vol. 2, p. 119.
[32] L. Bugayova, I. Gerus, A. Glushchenko, A. Dyadyusha, Y. Kurioz, V. Reshetnyak, Y. Reznikov, and J. West, Liq. Cryst. **29**, 209 (2002).
[33] A. Dyadyusha, A. Khizhnyak, T. Marusii, V. Reshetnyak, Y. Reznikov, and O. Yaroshchuk, Mol. Cryst. Liq. Cryst. Sci. Technol., Sect. A **263**, 339 (1995).
[34] O. Yaroshchuk, Y. Zakrevskyy, S. Kumar, J. Kelly, L. C. Chien, and J. Lindau, Phys. Rev. E **69**, 011702 (2004).